articles

molecular pharmaceutics

Biodistribution and Hepatic Uptake of Triplex-Forming Oligonucleotides against Type α1(I) Collagen Gene Promoter in Normal and Fibrotic Rats

Kun Cheng,[†] Zhaoyang Ye,[†] Ramareddy V. Guntaka,*[,‡] and Ram I. Mahato*[,†]

Departments of Pharmaceutical and Molecular Sciences, University of Tennessee Health Science Center, Memphis, Tennessee 38163

Received March 16, 2005

Abstract: Fibrosis is characterized by excessive production of extracellular matrix (ECM) components, predominantly type 1 collagen. Earlier we developed an antigene approach, using a type α1(I) promoter specific TFO to inhibit collagen gene expression. In this report, biodistribution and hepatic cellular and subcellular localization of the 25-mer antiparallel phosphorothioate triplex-forming oligonucleotide (APS TFO) were determined after intravenous injection into rats. TFOs distributed to all the major organs, with higher uptake in the liver, kidney, and spleen. The plasma concentration versus time profile of the ^{33}P-TFO was biphasic, with 4.36 min as $t_{1/2\alpha}$ of distribution and 34.6 min as $t_{1/2\beta}$ of elimination. TFO concentrations in the liver increased nonlinearly with increase in its dose from 0.2 to 50 mg/kg, but decreased when injected into fibrotic rats. Competition studies with polyinosinic acid (polyI) and dextran sulfate suggested the involvement of scavenger receptors in the hepatic uptake of the TFO. Intrahepatic cellular distribution by Kupffer, endothelial, and hepatic stellate cells (HSCs) accounted for almost 70% of the liver uptake of ^{33}P-TFO, while only 30% was associated with hepatocytes. The level of liver nuclei-associated TFO was much lower relative to that found in the cytoplasm at 2 and 4 h postinjection. TFO, however, inhibited collagen expression as evidenced by Sirius red staining of the liver section of fibrotic rats. In conclusion, systemic delivery of the TFO against type α1(I) collagen gene promoter may be used for the treatment of liver fibrosis.

Keywords: Liver fibrosis; triplex-forming oligonucleotide (TFO); hepatic stellate cells; liver perfusion; biodistribution; nuclear localization

Introduction

Fibrosis is a wound-healing response characterized by disproportionate accumulation of extracellular matrix (ECM) components, especially type I and III fibrillar collagens within the perivascular and interstitial space of tissues. This holds true in major pathologic states, such as liver fibrosis, progressive myocardial fibrosis, restenosis, pulmonary fibrosis, and keloids. Such fibrosis has been attributed to phenotypically transformed fibroblast-like cells, often termed myofibroblasts in myocardium, hepatic stellate cells (HSCs) in the liver, mesangial cells in the kidney, and lung fibroblasts in the lung.[1] Treatment of fibrosis requires specific delivery of antifibrotic agents to these fibroblast-like cells.

Liver fibrosis is a scarring response that results from chronic injury due to hepatitis B and C, excessive alcohol ingestion, nonalcoholic steatohepatitis, and iron overload. Fibrosis culminates in cirrhosis, the end stage leading to liver failure. Hence, a potent antifibrotic therapy is in urgent need to slow or reverse liver fibrosis. Regardless of the mechanism

* Corresponding authors. R.I.M.: 26 South Dunlap Street, Feurt 413, Memphis, TN 38163; tel, (901) 448-6929; fax, (901) 448-6092; e-mail, rmahato@utmem.edu. R.V.G.: 101 Molecular Science Building, Memphis, TN 38163; tel, (901) 448-8230; fax, (901) 448-8462; e-mail, rguntaka@utmem.edu.

[†] Department of Pharmaceutical Sciences.

[‡] Department of Molecular Sciences.

(1) Brenner, D. A.; Rippe, R. A.; Rhodes, K.; Trotter, J. F.; Breindl, M. *J. Lab. Clin. Med.* **1994**, *124*, 755−760.

10.1021/mp050012x CCC: $30.25
Published on Web 05/10/2005

of induction, fibrosis is due to the overproduction of type I collagen. Therefore, inhibition of transcription of type I collagen gene is expected to prevent fibrosis. Mammalian α1(I) collagen gene promoter contains two contiguous 30 bp polypurine tracts C1 and C2, located at −141 to −170 and −171 to −200 upstream from the transcription start site.[2] In our previous study, we have shown that the 25-mer antiparallel phosphorothioate (APS) TFOs specific for C1 formed triplexes efficiently and inhibited transcription in rat cells (∼50% of control).[2,3]

Having a thorough understanding of the disposition profiles of TFO is crucial for its effective therapeutic applications. Activated HSCs, residing in the perisinusoidal space of Disse in the liver, are the major source of type I collagen and other components of ECM.[4] Hepatic myofibroblasts are other fibrogenic cells that derive of portal and central veins, and periductular fibroblasts.[5] Excessive collagen production in the liver can be inhibited by triplex formation with type α1(I) collagen gene promoter. To achieve this goal, the TFO should be delivered to the liver in general and liver fibrogenic cells in particular. Although there are many reports about the biodistribution of antisense oligodeoxynucleotides (ODNs) at whole body and organ (liver and kidney) levels,[6−8] no information is available on ODN delivery to HSCs. Moreover, most biodistribution studies used phosphorothioate oligonucleotides (PS ODNs), which were not G-rich. PS ODNs containing four or more consecutive guanine residues form G-quartet structures and have a tendency to show nonspecific antiproliferative activity due to their binding to cellular protein nucleolin.[9,10] Therefore, it is important to thoroughly investigate the distribution of the TFO in different organs and different liver cell types.

In the present study, we investigated the pharmacokinetics and biodistribution of the ^{33}P-labeled 25-mer APS TFO after systemic administration into normal and liver fibrotic rats. Intrahepatic cellular distribution was also determined by collagenase liver perfusion after intravenous injection of ^{33}P-TFO followed by isolation of different liver cell types. Subcellular distribution of ^{33}P-TFO in nuclei, cytoplasm, and membranes of the liver was also determined. Finally, we determined the effect of TFO on liver fibrosis by Sirius red staining.

Experimental Section

Materials. The 25-mer APS TFO (5′ GGGA AGG AAA GGG AGG AGG GGG GAG 3′) was purchased from The Midland Certified Reagent Company Inc. (Midland, TX). [γ-^{33}P]-ATP was obtained from MP Biomedicals (Irvine, CA). T4 polynucleotide kinase was purchased from New England Biolabs (Beverly, MA). Bio-Gel P-6DG gel was procured from Bio-Rad Laboratories (Hercules, CA). Soluene-350 (tissue solubilizer) and Hionic-Fluor (scintillation fluid) were purchased from Perkin-Elmer (Boston, MA). Isoflurane was obtained from Baxter Health Corporation (Deerfield, IL). Type IV collagenase was purchased from Worthington Biochemical Corporation (Lakewood, NJ). Dimethylnitrosamine (DMN), Pronase, polyinosinic acid (polyI, MW 160 000−1 000 000) and polycytidylic acid (polyC, MW 170 000−1 900 000) were purchased from Sigma-Aldrich, Co. (St. Louis, MO). Dextran sulfate (MW 500 000) was purchased from Pharmacia Fine Chemicals (Uppsala, Sweden) and Nycodenz AG from Greiner Bio-One Inc. (Longwood, FL). PE-60 polyethylene tubing was purchased from Becton Dickinson and Company (Sparks, MD), and heparin solution was procured from American Pharmaceutical Partners, Inc. (Los Angeles, CA). Direct Red 80 (Sirius red) and Nuclei PURE Prep Nuclei Isolation Kit were purchased from Sigma-Aldrich (St. Louis, MO).

Labeling of TFO. The 25-mer APS TFO was labeled by adding γ-^{33}P to the 5′ end using [γ-^{33}P]-ATP and T4 polynucleotide kinase. Unincorporated [γ-^{33}P]-ATP was removed from radiolabeled TFO by size exclusion chromatography with Bio-Gel P-6DG gel (Bio-Rad Laboratories, Hercules, CA). The incorporation efficiency of the purified ^{33}P-TFO was determined by the trichloroacetic acid (TCA) precipitation method, and the value was more than 95%. The specific activity of the labeled TFO was about 5×10^5 to 10×10^5 cpm/μg. Radioactivity was measured on a TRI-CARB 2000 liquid scintillation analyzer (PACKARD Instrument Company, Meridon, CT).

Stability of ^{33}P-TFO. The stability of ^{33}P-TFO was determined in rat serum and liver lysates. For the serum stability, 10 μL of ^{33}P-TFO (0.1 mg/mL) was incubated with 10 μL of rat serum for 1, 2, 4, 6, and 24 h at 37 °C, loaded onto 20% polyacrylamide gels, and run at 85 V for 90 min. For stability of TFO in liver lysate, 500 mg of fresh rat liver was homogenized in 4 mL of ice cold lysis buffer (10 mM NaCl, 20 mM Tris HCl, 10 mM EDTA, and 0.1% Triton X-100). The homogenized liver suspension was centrifuged at 12 000 rpm for 15 min, and supernatant was used as the liver lysate for the stability study. Fifteen microliters of ^{33}P-TFO (0.1 mg/mL) was incubated with 5 μL of liver lysate for 1, 2, 3, 4, 5, 6, and 24 h at 37 °C. The samples were

(2) Joseph, J.; Kandala, J. C.; Veerapanane, D.; Weber, K. T.; Guntaka, R. V. *Nucleic Acids Res.* **1997**, *25*, 2182−2188.
(3) Nakanishi, M.; Weber, K. T.; Guntaka, R. V. *Nucleic Acids Res.* **1998**, *26*, 5218−5222.
(4) Friedman, S. L. *J. Biol. Chem.* **2000**, *275*, 2247−2250.
(5) Knittel, T.; Kobold, D.; Saile, B.; Grundmann, A.; Neubauer, K.; Piscaglia, F.; Ramadori, G. *Gastroenterology* **1999**, *117*, 1205−1221.
(6) Zhang, R.; Diasio, R. B.; Lu, Z.; Liu, T.; Jiang, Z.; Galbraith, W. M.; Agrawal, S. *Biochem. Pharmacol.* **1995**, *49*, 929−939.
(7) Mahato, R. I.; Takemura, S.; Akamatsu, K.; Nishikawa, M.; Takakura, Y.; Hashida, M. *Biochem. Pharmacol.* **1997**, *53*, 887−895.
(8) Graham, M. J.; Crooke, S. T.; Monteith, D. K.; Cooper, S. R.; Lemonidis, K. M.; Stecker, K. K.; Martin, M. J.; Crooke, R. M. *J. Pharmacol. Exp. Ther.* **1998**, *286*, 447−458.
(9) Bates, P. J.; Kahlon, J. B.; Thomas, S. D.; Trent, J. O.; Miller, D. M. *J. Biol. Chem.* **1999**, *274*, 26369−26377.
(10) Xu, X.; Hamhouyia, F.; Thomas, S. D.; Burke, T. J.; Girvan, A. C.; McGregor, W. G.; Trent, J. O.; Miller, D. M.; Bates, P. J. *J. Biol. Chem.* **2001**, *276*, 43221−43230.

loaded onto 20% polyacrylamide gels for electrophoresis, followed by autoradiography.

Biodistribution of TFO. The animal protocol was approved by the Animal Care and Use Committee (ACUC), Department of Comparative Medicine, University of Tennessee Health Science Center, Memphis, TN 38163. Male Sprague−Dawley rats (Harlan Co., San Diego, CA) weighing 150 g were used in this study, and 4 rats were used for each time point. Unlabeled and ^{33}P-labeled TFO were mixed in saline to give a final concentration of 1 mg/mL. Rats were anesthetized by inhalation of isoflurane, and TFO was injected via tail vein at a dose of 1 mg/kg of body weight. At various time points, 0.5 mL of blood was collected by cardiac puncture in heparinized tubes, and urine was collected directly from the bladder via a 0.26 gauge needle syringe. The animals were then sacrificed, and major tissues (liver, kidney, spleen, heart, lung, and muscle) were collected, washed, blotted dry, weighed, and stored at −80 °C. The radioactivity of the urine sample was counted directly after addition of 10 mL of scintillation fluid. One hundred fifty microliters of plasma and 150 mg of each tissue were incubated with 2 mL of tissue solubilizer for 3 h at 55 °C and overnight at room temperature. Three hundred fifty microliters of H_2O_2 was added and incubated at 55 °C for another 30 min. Ten milliliters of scintillation fluid was added to each sample, and the radioactivity was counted using a liquid scintillation counter.

Determination of Pharmacokinetic Profiles. Plasma data was analyzed using WinNonlin Professional (version 4.0.1, Pharsight Corporate., Mountainview, CA). The TFO plasma concentration data versus time were fitted using one- and two-compartment models, and pharmacokinetic parameters were calculated: area under the curve (AUC), C_{max}, T_{max}, and clearance (CL). The data were best fitted to a two-compartment model where

$$C_t = A\,e^{-\alpha t} + B\,e^{-\beta t}$$

and C_t equals concentration at time t, A and B are the y-axis intercepts, and α and β are the hybrid constants for distribution and elimination, respectively.

Tissue distribution data of ^{33}P-TFO were analyzed in terms of a clearance and a tissue uptake rate index using biexponential equations as described previously.[7] The change in the amount of radioactivity in a tissue with time can be described as follows:

$$dT(t)/t = CL_{in}C(t) - K_{out}T(t) \quad (1)$$

where $T(t)$ (% of dose/g) represents the amount of radioactivity in 1 g of the tissue, $C(t)$ (% of dose/mL) is the plasma concentration of radioactivity, CL_{in} (mL h^{-1} g^{-1}) is the tissue uptake rate index from the plasma to the tissue, and K_{out} (1/h) is the rate constant for efflux from the tissue. In the present study, the efflux process can be considered negligible during the initial time points up to 60 min. Hence, eq 1 integrates to

$$CL_{in} = T(t_1)\int_0^{t_1} C(t_1)\,dt = T(t_1)/AUC_{0-t_1} \quad (2)$$

where t_1 (h) is the sampling time. According to eq 2, the tissue uptake rate index is calculated using the amount of radioactivity in the tissue at an appropriate interval and the area under the plasma concentration−time curve (AUC) up to the same time point. Then, the organ clearance (CL_{org}) is expressed as follows:

$$CL_{org} = CL_{in}W \quad (3)$$

where W (g) is the total weight of the organ. When the tissue uptake process followed nonlinear kinetics, CL_{in} values would represent an average value for the overall experimental period. Total body clearance (CL_{total}) was calculated from AUC for infinite time (AUC_∞) by the following equation:

$$CL_{total} = dose/AUC_\infty \quad (4)$$

The tissue uptake clearance and index were calculated using the values up to 30 min after injection, assuming that TFOs were fairly stable within this period.

Induction of Liver Fibrosis. Liver fibrosis was induced by intraperitoneal injections of dimethylnitrosamine (DMN) into rats at a dose of 1 mL (1% in saline)/kg of body weight. This is a well-established animal model for liver fibrosis which has pathophysiological properties similar to those of human liver fibrosis.[11,12] Injections were given on the first three consecutive days of each week over a 3 week period. After the DMN injection for 3 weeks, 3 rats were killed for examination of liver fibrosis development and measurement of hydroxyproline content as described by Jamall et al.[13] After 3 weeks of treatment, rats were used for biodistribution studies.

Competition in Hepatic Uptake of TFO. One minute before the injection of ^{33}P-TFO at a dose of 1 mg/kg (specific activity: 1×10^6 cpm/mL), the rats received one of the following polyanions: 10 mg/kg polyinosinic acid (polyI), 10 mg/kg polycytidylic acid (polyC), 20 mg/kg dextran sulfate. At 30 min postinjection, 0.5 mL of blood was collected by cardiac puncture, the liver was harvested, and the radioactivity was determined as described above.

Liver Perfusion. Rats (200−250 g) were anesthetized by inhalation of isoflurane, 100 IU of heparin was injected via tail vein, the abdomen was opened, and the portal vein was cannulated with a PE-60 polyethylene tube. The liver was first perfused with 2 mL of diluted heparin solution at 20 units/mL to avoid blood clogging in the liver. The liver was preperfused in situ with 200 mL of Ca^{2+}/Mg^{2+}-free Hanks' balanced salt solution at a flow rate of 15 mL/min, and was then perfused with Hanks' balanced salt solution containing

(11) Jezequel, A. M.; Mancini, R.; Rinaldesi, M. L.; Macarri, G.; Venturini, C.; Orlandi, F. *J. Hepatol.* **1987**, *5*, 174−181.
(12) Jenkins, S. A.; Grandison, A.; Baxter, J. N.; Day, D. W.; Taylor, I.; Shields, R. *J. Hepatol.* **1985**, *1*, 489−499.
(13) Jamall, I. S.; Finelli, V. N.; Que Hee, S. S. *Anal. Biochem.* **1981**, *112*, 70−75.

0.05% type IV collagenase and 0.1% Pronase for an additional 250 mL at a flow rate of 10 mL/min. All the perfusion solutions were incubated at 37 °C.

After perfusion, the liver was removed and immersed in Hanks' balanced salt solution, and all the extraneous tissue was cut away without damage to the capsule. The capsule was disturbed, and the cells were freed into the medium by mild agitation with forceps. The suspension was passed through sterilized gauze, and the cell suspension was centrifuged at 50*g* for 5 min; the pellet containing hepatocytes was resuspended in Hanks' buffer, and viability was determined by trypan blue staining. The supernatant which was enriched in nonparenchymal cells was further centrifuged at 100*g* for 5 min to remove residual parenchymal cells. Nonparenchymal cells were collected by centrifugation of the supernatant at 500*g* for 10 min. HSCs were further separated from Kupffer and endothelial cells via the gradient method as described by Hendriks et al.[14] To generate a gradient, collected nonparenchymal cells were dispersed in 10 mL of Nycodenz solution at 11.5%. Under part of the gradient 5 mL of 17.5% Nycodenz solution was layered, and these two solutions were overlaid with 2 mL of PBS. This gradient was then spun at 1450*g* for 17 min with a slow acceleration and deceleration. After centrifugation, the top of the second layer (11.5%) contains purified HSCs and the top of the 17.2% layer contains Kupffer and endothelial cells. The purity of isolated HSCs was determined by autofluorescence and immunostaining for desmin, which is an intermediate filament specific for stellate cells. Separated cells were counted, and 10×10^6 of each cell type was digested with Soluene-350 overnight. Hionic-Fluor was added, and the radioactivity was determined using a liquid scintillation counter.

Subcellular Distribution of ^{33}P-TFO in the Liver. Unlabeled and ^{33}P-labeled TFO were mixed in saline to give a final concentration of 1 mg/mL. Rats were anesthetized by inhalation of isoflurane, and TFO was injected via tail vein at a dose of 1 mg/kg of body weight. At 2 and 4 h postinjection, the animals were sacrificed and the livers were collected, washed, blotted dry, and stored at −80 °C. One gram of fresh liver was used for isolation of nuclei according to the supplier's protocol (Sigma Aldrich, St. Louis, MO). The purity and number of isolated nuclei was determined under microscopy by dilution in trypan blue solution. The yield of nuclei was calculated to be 42−45% by comparing the number of isolated nuclei to the starting cell number. Isolated nuclei were digested with Soluene-350 overnight. Hionic-Fluor was added, and the radioactivity was determined using a liquid scintillation counter. The percentage of nuclear uptake of the TFO in the liver was calculated as TFO_{nuclei}/TFO_{liver}.

Effect of TFO on Liver Fibrosis. DMN-induced fibrotic rats were used to determine the effect of TFO on liver fibrosis. DMN was injected intraperitoneally into rats at a dose of 1 mL (1% in saline)/kg of body weight for 3 consecutive days per week for 5 weeks. TFO was injected intraperitoneally at 4 mg/kg of body weight every alternate day from the second week. After 5 weeks, all rats were sacrificed, and pieces of liver were harvested, fixed in 10% formalin, embedded in paraffin, cut into 5 μm sections, and placed onto slides. The slides were deparaffinized, and the sections were stained with 0.1% Sirius red in saturated picric acid solution at pH 2.

Statistical Analysis. Data were expressed as the mean ± standard deviation (SD). The difference between any two groups was determined by ANOVA. $P < 0.05$ was considered statistically significant.

Results

G-Quartet Formation and Stability of ^{33}P-TFO. The TFO we used contains GGGGGG which has the potential to form guanine quartet containing structures (G quartets) and may provide resistance to nuclease.[15] PS ODNs containing 4 or more consecutive guanosine residues have a tendency to show some nonspecific effects including antiproliferative activity due to binding to cellular protein nucleolin.[16] Therefore, we heated TFO in boiling water and then cooled it in ice water to remove the G quartet of the TFO. As shown in Figure 1A, the G quartets disappeared after heating with little effect on the stability of ^{33}P-TFO.

Following labeling of TFO with [γ-^{33}P]-ATP and purification by size exclusion chromatography, the stability of ^{33}P-TFO was determined by incubating in the rat serum (Figure 1B) and liver lysate (Figure 1C) at 37 °C, followed by polyacrylamide gel electrophoresis and autoradiography. As shown in Figure 1B,C, the labeled TFO was fairly stable in the rat serum for 6 h and liver lysate up to 24 h postincubation. A small amount of the ^{33}P-TFO appeared to bind to proteins in the liver lysate.

In Vivo Disposition. Following intravenous injection of ^{33}P-TFOs into rats, ^{33}P-TFOs were eliminated rapidly from circulation and accumulated in all peripheral tissues, with the highest uptake by the liver, spleen, and kidney, but very low levels in skeletal muscle (Figure 2A). Peak concentration of radioactivity was observed in the liver at 90 min after administration of ^{33}P-TFO.

Plasma elimination was biphasic with a distribution half-life ($t_{1/2\alpha}$) of 4.36 min and an elimination half-life ($t_{1/2\beta}$) of 34.6 min. Figure 2B summarizes the pharmacokinetic parameters such as the AUC, V_d, MRT, and CL_{org} for representative tissues calculated using biexponential equations. Consistent with rapid clearance (0.3153 ± 0.0167 mL/min), the TFO had large V_d of 14.14 ± 0.92 mL. Table 1 summarizes the tissue uptake rate index and organ clearance

(14) Hendriks, H. F.; Brouwer, A.; Knook, D. L. *Methods Enzymol.* **1990**, *190*, 49−58.

(15) Burgess, T. L.; Fisher, E. F.; Ross, S. L.; Bready, J. V.; Qian, Y. X.; Bayewitch, L. A.; Cohen, A. M.; Herrera, C. J.; Hu, S. S.; Kramer, T. B. *Proc. Natl. Acad. Sci. U.S.A.* **1995**, *92*, 4051−4055.

(16) Jason, T. L.; Koropatnick, J.; Berg, R. W. *Toxicol. Appl. Pharmacol.* **2004**, *201*, 66−83.

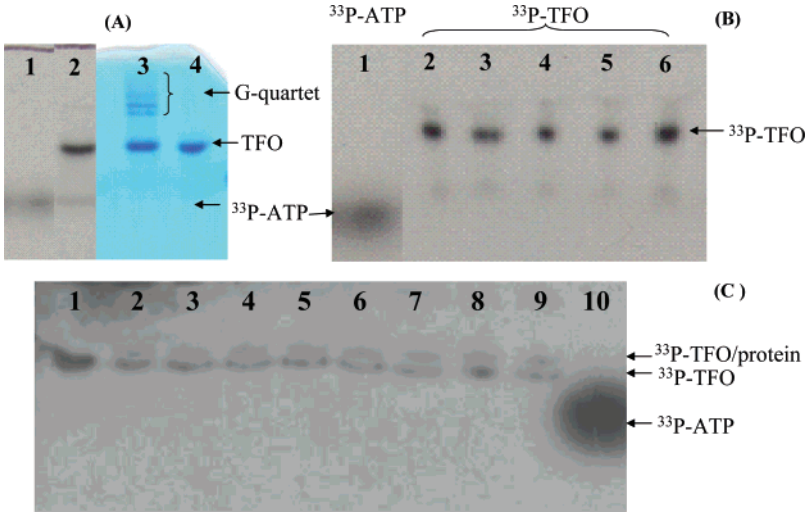

Figure 1. Determination of G-quartet formation (A) and stability of TFO in rat serum (B) and liver lysate (C). Samples were electrophoresed on 20% polyacrylamide gel and autoradiographed. (A) Lane 1: ^{33}P-ATP. Lane 2: ^{33}P-TFO. Lane 3: TFO without heating. Lane 4: TFO heated in boiling water. Lanes 3 and 4 were stained with methylene blue. (B) Stability of ^{33}P-TFO in rat serum. Lane 1: free ^{33}P-ATP. Lane 2: ^{33}P-TFO at 0 h. Lane 3: ^{33}P-TFO at 1 h. Lane 4: ^{33}P-TFO at 2 h. Lane 5: ^{33}P-TFO at 4 h. Lane 6: ^{33}P-TFO at 6 h of incubation in the rat serum at 37 °C. (C) Stability of ^{33}P-TFO in rat liver lysate. Lane 1: ^{33}P-TFO. Lane 2: ^{33}P-TFO at 0 h. Lane 3: ^{33}P-TFO at 1 h. Lane 4: ^{33}P-TFO at 2 h. Lane 5: ^{33}P-TFO at 3 h. Lane 6: ^{33}P-TFO at 4 h. Lane 7: ^{33}P-TFO at 5 h. Lane 8: ^{33}P-TFO at 6 h. Lane 9: ^{33}P-TFO at 24 h of incubation in the rat liver lysate at 37 °C. Lane 10: free ^{33}P-ATP.

of ^{33}P-TFO administered intravenously into rats at a dose of 1 mg/kg. The liver had the highest tissue uptake rate index (1800.75 μL h^{-1} g^{-1}) and CL_{org} (12 365.32 μL/h). The kidney was in the second place with the tissue uptake rate index of 1176.16 μL h^{-1} g^{-1} and CL_{org} of 1334.65 μL/h.

The levels of TFO concentration in the liver and other organs increased as the dose was escalated (Figure 3A). At doses of 0.2, 1, 10, and 50 mg/kg, the measured TFO levels were 2.34, 9.86, 53.55, and 115.58 ng/mg of liver tissue, respectively. An increase in TFO concentration was also seen in all other organs and in plasma (Figure 3A).

A saturation curve was obtained by plotting hepatic TFO concentration against the dose (Figure 3B). Nonlinear regression was then used to fit with the equation $C = C_{max}\cdot\text{Dose}/(K_m + \text{Dose})$, where C is the TFO concentration in the tissue, C_{max} is the maximum TFO concentration in the tissue, and K_m is the saturation constant. Hepatic uptake data (Figure 3B) showed a good fitting with the equation, but data for other organs did not. Saturation kinetics indicates that the hepatic uptake of TFO is receptor mediated in the range of 0.2−50 mg/kg. The K_m for liver was 19.771 mg/kg, indicating a stronger affinity of TFO with the receptor in the liver.

Effect of Fibrosis on Biodistribution of TFO. Fibrosis results in scar formation and changes in the subendothelial space of Disse and sinusoid, which may affect the hepatic uptake of the TFO.[4] Therefore, we determined the biodistribution at 30 min post systemic administration of ^{33}P-TFO in DMN-induced liver fibrotic rats. The hepatic uptake of ^{33}P-TFO decreased from 43% to 33%, while the plasma concentration increased from 15% to 26% at 30 min postinjection (Figure 4A). Similarly, at 4 h postinjection, the hepatic uptake of TFO decreased from 38% to 27% and the plasma concentration increased from 0.78% to 1.75% (Figure 4B). Compared to the normal rats, a significant increase in TFO concentration was observed in the kidney, heart, spleen, and lung at 30 min and 4 h postinjection of ^{33}P-TFO in the liver fibrotic rats (Figure 4).

Competition in Hepatic Uptake of TFO. The role of scavenger receptor on biodistribution of ^{33}P-TFO in rats was assessed by the effect of polyanions on the accumulation of radioactivity by selected tissues. Prior administration of polyanions such as polyI and dextran sulfate caused a significant decrease in the hepatic uptake, but that of polyC had little effect on the biodistribution of the TFO (Figure 5) at 30 min postinjection, suggesting the involvement of a type I/II scavenger receptor in their hepatic uptake.[17]

Isolation and Cultivation of Hepatic Stellate Cells. HSCs constitute less than 8% of the total liver cells, but have numerous vital functions including the storage and metabolism of vitamin A and ECM formation upon activation due to liver injury.[4] Therefore, we isolated HSCs by perfusing rat liver with a mixture of 0.05% collagenase and 0.1% Pronase followed by fractionation on Nycodenz gradient.[14] The purity of isolated HSCs was determined by vitamin A autofluorescence and staining with desmin antibodies. Figure 6 shows the morphology of hepatocytes, Kupffer and endothelial cells, and HSCs soon after isolation (A, C, E) and after 2 weeks of culturing (B, D, F). There was little

(17) Acton, S. L.; Scherer, P. E.; Lodish, H. F.; Krieger, M. *J. Biol. Chem.* **1994**, *269*, 21003−21009.

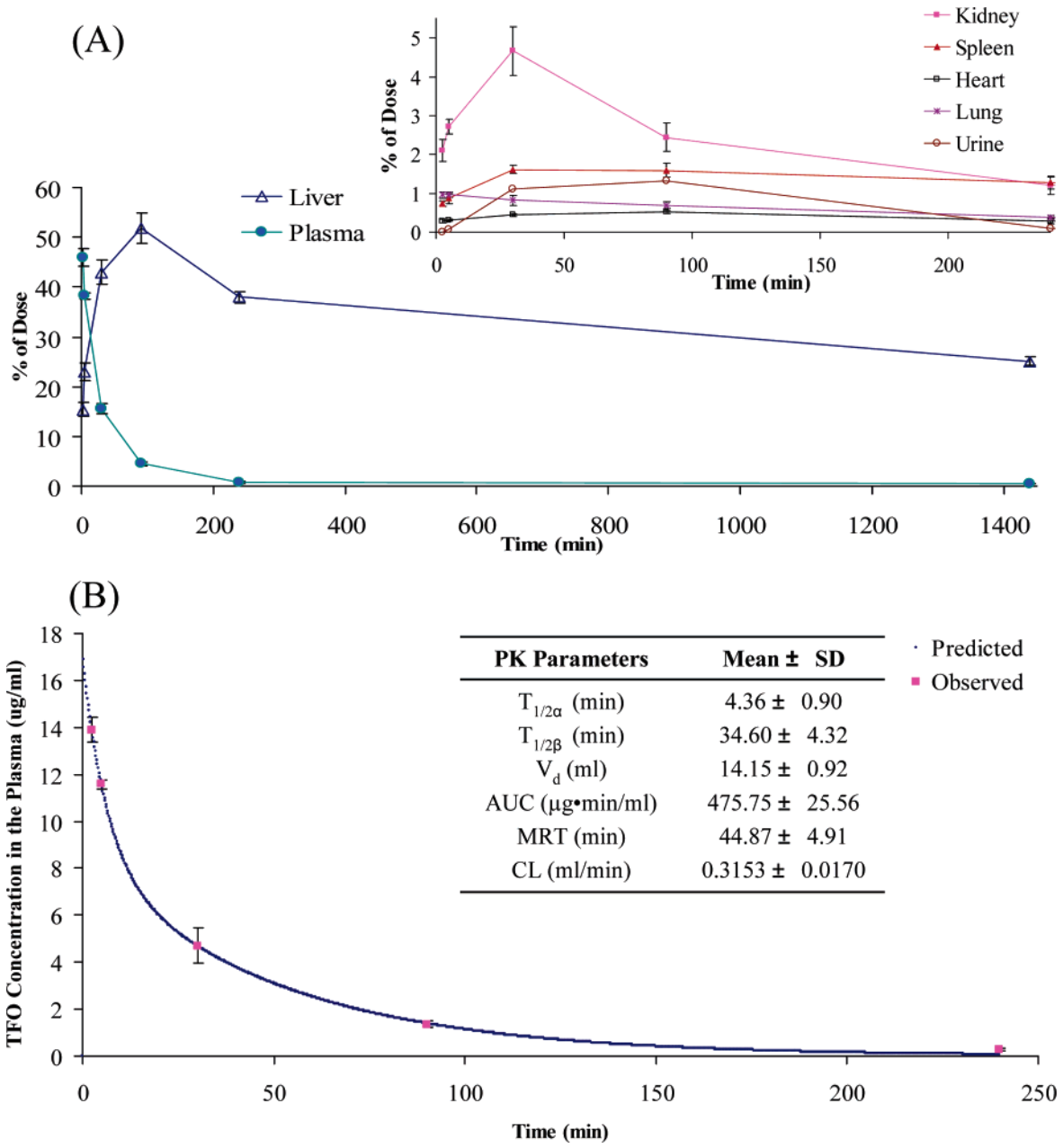

Figure 2. (A) Tissue accumulation and (B) plasma concentration of TFO after intravenous injection of a mixture of ^{33}P-TFO and TFO in rats at a dose of 1 mg/kg. At 2.5, 5, 30, 90, 240, and 1440 min after injection, blood was collected by cardiac puncture and urine was collected from the bladder. The rats were sacrificed, tissues were collected, washed, and weighed, 200 mg of tissue was digested, and radioactivity was determined using a scintillation counter. Plasma data was analyzed using a two-compartment model with WinNonlin Professional (version 4.0.1) software. Data are represented as the mean ± SD (n = 4).

Table 1. Tissue Uptake Rate Index and Clearance of ^{33}P-TFO Administered Intravenously into Rats at a Dose of 1 mg/kg (n = 4)

	tissue uptake rate index (μL h^{-1} g^{-1})	organ clearance (μL/h)
liver	1880.75 ± 191.68	11090.43 ± 1028.42
kidney	1176.16 ± 146.93	1204.99 ± 205.39
heart	243.81 ± 17.08	114.79 ± 9.68
spleen	1023.63 ± 48.19	414.24 ± 36.59
lung	276.42 ± 44.49	211.04 ± 42.18

contamination of other liver cells, and these HSCs were viable. Isolated HSCs elongated with culturing and displayed like myofibroblastic phenotype (Figure 6D).

Hepatic Cellular Localization. Since the liver represents a major site for TFO deposition after systemic administration, we perfused the liver at 30 min post ^{33}P-TFO administration at doses of 0.2 and 1 mg/kg and isolated different liver cells as described above. Substantial differences in the uptake of ^{33}P-TFO by different liver cells were evident (Figure 7). Although the percentage of the total liver recovery was similar for hepatocytes and HSCs (Figure 7B), the TFO concentration (ng/mg of cell protein) was in the following order: HSCs ≥ Kupffer and endothelial cells ≫ hepatocytes (Figure 7A). As expected, the TFO concentration in these

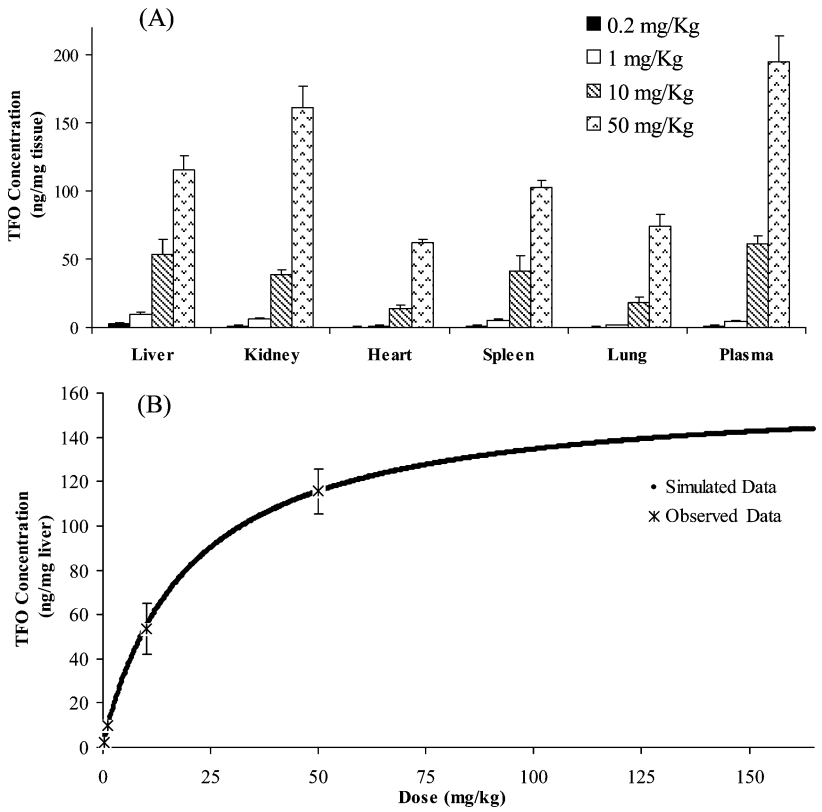

Figure 3. (A) Effect of dose on TFO concentrations in various tissues at 30 min after intravenous injection of a mixture of ^{33}P-TFO and TFO in rats. Blood was collected in heparinized tubes by cardiac puncture, and urine was collected from the bladder. The rats were sacrificed, tissues were collected, washed, and weighed, 200 mg of tissue was digested, and radioactivity was determined using a scintillation counter. Dose: 0.2, 1, 10, and 50 mg/kg. Data are represented as the mean ± SD ($n = 5$). (B) Saturation plot of hepatic uptake of ^{33}P-TFO. The hepatic uptake vs dose data were used for fitting to the equation of $C = C_{max}\cdot\text{Dose}/(K_m + \text{Dose})$ to obtain a saturation kinetic constant K_m of 19.722 mg/kg and a maximal TFO concentration in the liver C_{max} of 161.1 ng/mg of liver.

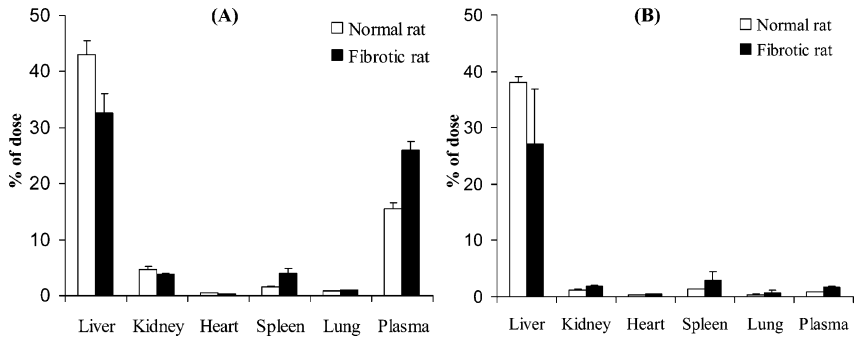

Figure 4. Effect of liver fibrosis on biodistribution of TFO. At (A) 30 min and (B) 240 min after intravenous injection of ^{33}P-TFO into normal and fibrotic rats at a dose of 1 mg/kg, blood was collected by cardiac puncture and urine was collected from the bladder. The rats were sacrificed, tissues were collected, washed, and weighed, 200 mg of tissue was digested, and radioactivity was determined using a scintillation counter. Data are represented as the mean ± SD ($n = 5$).

cells significantly increased when the dose was increased from 0.2 to 1 mg/kg. In liver fibrotic rats, the percentage of total liver uptake by the hepatocytes was higher but lower by Kupffer and endothelial cells compared to those observed in the normal rats (Figure 7B). However, it is important to note that liver perfusion of fibrotic rats was very difficult and required perfusion with 0.05% collagenase and 0.1% Pronase for an additional 20−30 min. Thus, it is possible that % of the liver uptake by hepatocytes of the fibrotic rats might have been overestimated due to possible contamination of some nonparenchymal cells in the hepatocyte preparations.

Subcellular Distribution of ^{33}P-TFO in the Liver. To inhibit the transcription of type α1(I) collagen, TFO must enter the nucleus and form triple helices with the genomic DNA. Therefore, we isolated the nuclei from rat liver at 2 and 4 h after systemic administration of ^{33}P-TFO. Fraction-

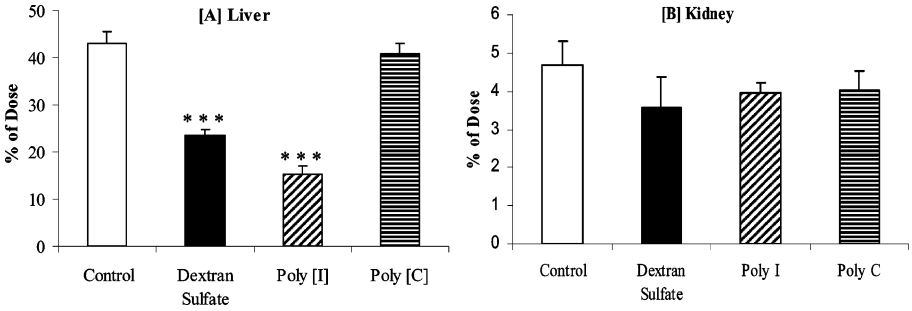

Figure 5. Effect of polyanions on ^{33}P-TFO accumulation in (A) the liver and (B) the kidney at 30 min after intravenous injection in rats at a dose of 1 mg/kg. One minute after intravenous injection of polyI (10 mg/kg), polyC (10 mg/kg), or dextran sulfate (20 mg/kg), ^{33}P-TFO was administered in a similar manner. Blood was collected by cardiac puncture in heparinized tubes and urine was collected from the bladder. The animals were sacrificed, tissues were collected, washed, and weighed, 200 mg of tissue was digested, and radioactivity was determined using a scintillation counter. Plasma and tissue accumulation of radioactivity were compared with those of the control samples at 30 min after injection. Data are presented as the mean ± SD ($n = 5$). *** represents statistical significance at 0.005.

ation by sucrose gradient gave fairly pure and intact nuclei (Figure 8A) with a recovery of 42−45%. The majority of the TFO stayed in the cytoplasm of liver cells, and the TFO uptake in the nuclei was only 3.77 ± 0.44% and 6.28 ± 0.59% of the total hepatic uptake of TFO at 2 and 4 h, respectively (Figure 8B). However, it is important to note that only 42−45% of the cell nuclei could be isolated. Therefore, the actual nuclear distribution of the TFO could be as high as 9.52 ± 2.04% and 14.11 ± 2.04% at 2 and 4 h, respectively.

Effect of TFO on Liver Fibrosis. To determine the effect of the TFO on liver fibrosis, DMN-induced fibrotic rats received TFO every alternate day from the second week of DMN treatment. Hepatic collagen deposition/accumulation was determined by Sirius red staining of the liver sections (Figure 9A). Collagen was mainly deposited in the space of Disse, and moderate to severe collagen deposition was observed with the DMN-treated rats (Figure 9B). Control rats (Figure 9C) showed much lower collagen deposition in the liver compared to that of the DMN-treated rats. TFO treated rats showed higher collagen deposition than that of the controlled rats, but much lower than that of the DMN-treated rats, suggesting that the TFO can inhibit collagen synthesis in the liver.

Discussion

Systemic delivery of ODNs is promising for the treatment of both genetic and acquired diseases. PS ODNs are by far the most extensively studied, and significant progress has been made which resulted in one commercial product (Vitravene) as well as several promising clinical trials. Antisense ODNs have been shown to inhibit type α1(I) collagen gene expression in NIH 373 cells in culture.[18] Compared to quiescent HSCs, activated HSCs contain 60−70-fold more collagen α1(I) mRNA.[19] Transfection of activated HSCs with molecular decoy and small interfering double-stranded RNA (siRNA) has been shown to significantly decrease α1(I) collagen mRNA.[19,20] However, no attempt was made to deliver these ODNs and siRNA to liver fibrogenic cells in vivo. Although systemic administration of siRNA against Fas or Caspase 8 has shown promise in controlling liver fibrosis,[21,22] high-volume hydrodynamic administration is not feasible in a clinical setting.

One of the main advantages of the TFO over antisense ODNs and siRNA is that it targets two alleles of the target gene existing per cell rather than mRNA, which is usually present in hundreds or thousands of copies per cell. The TFO we work with is unique in at least two aspects: first, it is polypurine TFO without any CpG motif; and second, it forms triplex under physiological conditions. We have previously shown that the 25-mer APS TFO could form triplex with duplex DNA of the C1 region (−170 to −141) of the α1 (I) collagen gene promoter and effectively inhibit its transcription in vitro.[2,3] Thus, the TFO against α1(I) collagen can be used as a potent antifibrotic drug. In this study, we determined the biodistribution at whole body, organ (liver), cellular, and subcellular levels of the TFO after systemic administration in both normal and liver fibrotic rats.

The plasma kinetic disposition of ^{33}P-TFO was characterized by rapid distribution to tissues (Figure 2), which is in good agreement with the disposition profiles of PS and G-rich ODNs reported in the literature.[23−27] A dose-dependent increase in TFO concentrations in the tissues was observed

(18) Laptev, A. V.; Lu, Z.; Colige, A.; Prockop, D. J. *Biochemistry* **1994**, *33*, 11033−11039.

(19) Stefanovic, B.; Schnabl, B.; Brenner, D. A. *J. Biol. Chem.* **2002**, *277*, 18229−18237.

(20) Lindquist, J. N.; Parsons, C. J.; Stefanovic, B.; Brenner, D. A. *J. Biol. Chem.* **2004**, *279*, 23822−23829.

(21) Song, E.; Lee, S. K.; Wang, J.; Ince, N.; Ouyang, N.; Min, J.; Chen, J.; Shankar, P.; Lieberman, J. *Nat. Med.* **2003**, *9*, 347−351.

(22) Zender, L.; Hutker, S.; Liedtke, C.; Tillmann, H. L.; Zender, S.; Mundt, B.; Waltemathe, M.; Gosling, T.; Flemming, P.; Malek, N. P.; Trautwein, C.; Manns, M. P.; Kuhnel, F.; Kubicka, S. *Proc. Natl. Acad. Sci. U.S.A.* **2003**, *100*, 7797−7802.

(23) Yu, R. Z.; Geary, R. S.; Monteith, D. K.; Matson, J.; Truong, L.; Fitchett, J.; Levin, A. A. *J. Pharm. Sci.* **2004**, *93*, 48−59.

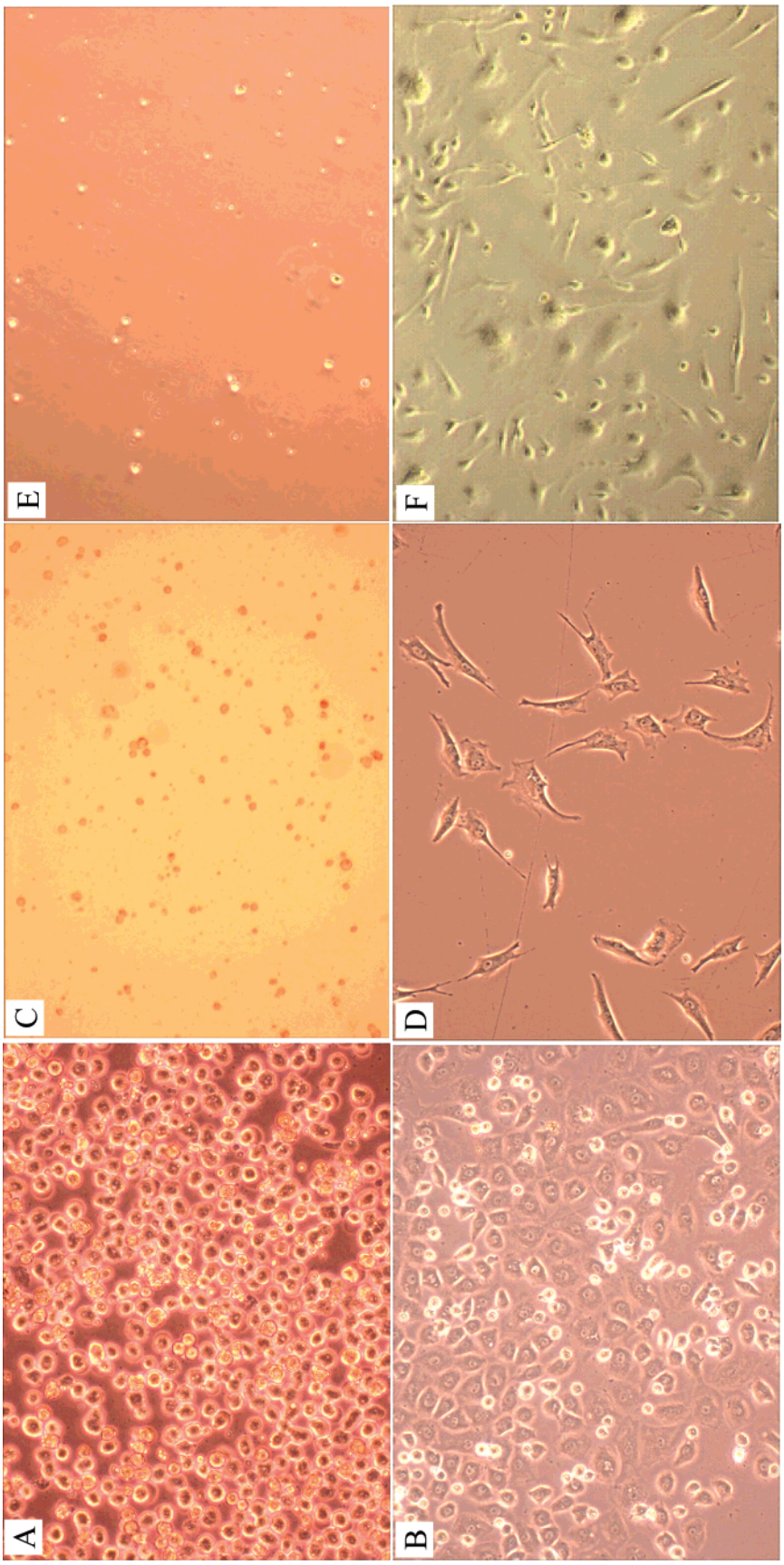

Figure 6. Morphology of different liver cells after in situ liver perfusion with a mixture of 0.05% collagenase and 0.1% Pronase and fractionation on Nycodenz gradient: (A, C, E) freshly isolated liver cells; (B, D, F) isolated liver cells after 2 weeks of culturing.

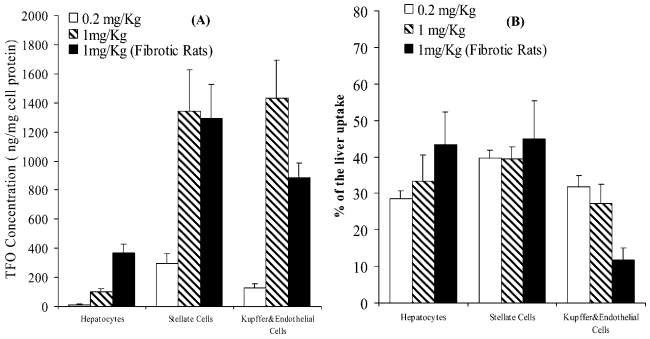

Figure 7. Hepatic cellular localization of ^{33}P-TFO at 30 min after intravenous administration in normal and fibrotic rats at doses of 0.2 and 1 mg/kg. Different liver cells were isolated by in situ liver perfusion with a mixture of 0.05% collagenase and 0.1% Pronase and fractionation on Nycodenz gradient. The amount of TFO found in each cell type is given as (A) ng/mg of cell protein and (B) % of the total liver recovery. Data are presented as the mean ± SE ($n = 4$).

(Figure 3A). Consistent with the literature,[8,28,29] the hepatic uptake of the TFO was linear at low doses (0.2−1 mg/kg), but nonlinear at higher doses (above 1 mg/kg) (Figure 3B). A saturation kinetic equation, $C = C_{max}\cdot\text{Dose}/(K_m + \text{Dose})$, was well fitted with the hepatic uptake of the TFO versus dose, indicating a receptor-mediated mechanism for the TFO uptake in the liver. Saturable uptake of the TFO in organs of higher affinity results in redistribution of the ODNs to other organs.[30]

Fibrosis results in the deposition of excessive fibrous or collagenous proteins in the subendothelial space or space of Disse. This, in turn, results in decreased free exchange flow between hepatocytes and sinusoidal blood.[31] In the DMN-induced liver fibrotic rats, the hepatic accumulation of the TFO decreased from 43% to 33% at 30 min (Figure 4A) and 38% to 27% at 4 h (Figure 4B) postinjection.

Involvement of scavenger receptors in the hepatic uptake of PS ODNs has been reported.[25,32−34] In the present study, prior injection of polyI and dextran sulfate inhibited the hepatic uptake, but not the renal uptake of ^{33}P-TFO (Figure 5). Steward et al.[32] also reported that coadministration of dextran sulfate had little effect on the renal accumulation of ^{3}H-ODNs. Similarly, Yamasaki et al. (2002) demonstrated that the renal uptake of succinylated proteins was independent of scavenger receptor mediated endocytosis.[35] These authors suggested that the urinary excretion may effectively mask the scavenger receptor mediated tissue uptake of ODNs and prevent accurate explanation.[32] However, inhibition by polyI and dextran sulfate cannot be taken as definitive evidence of specific binding by the scavenger receptors because several other receptors and uptake mechanisms are also inhibited by these compounds.[36] Nevertheless, our data suggests that scavenger receptors may be involved in the hepatic uptake of TFO.

Competition results are in good agreement with our results of the dose effect on the hepatic uptake of the TFO. Both studies showed the receptor-mediated uptake of the TFO by the liver. Moreover, hepatic uptake of the TFO showed a good fit with a saturation kinetic equation (Figure 3B). We predicted the competition of polyI and dextran sulfate by constructing a mathematical model with two assumptions: (i) the uptake of TFO in the liver is mediated by scavenger receptor, and (ii) both dextran sulfate and polyI could bind to the scavenger receptor of the liver similarly to the TFO. Therefore the preinjected polyanions will inhibit the same number of TFO molecules to bind to the receptors in the liver. Prediction of the competition effect was calculated using the equation $U'_{TFO} = U_{TFO}[(Q_{TFO} - Q_{Inh})/Q_{TFO}]$, where U_{TFO} represents the % of the hepatic uptake of the TFO with no preinjection of polyanions, U'_{TFO} represents the % of the hepatic uptake of the TFO after preinjection of polyanions, and Q_{TFO} represents the number of TFO molecules, while Q_{Inh} represents the number of preinjected polyanions. The theoretical values of the hepatic uptake of the TFO were 29% and 21% when dextran sulfate and polyI were preinjected. These values are close to the observed values, 23.57% for dextran sulfate and 15.28% for polyI.

We and others have previously reported that the hepatic uptake of PS ODNs is mainly due to liver nonparenchymal cells.[14,37] Biessen et al. (1998) demonstrated that ^{32}P-ODN uptake by different liver cell types is influenced by its G contents and its binding to both Kupffer and endothelial cells

(24) Agrawal, S.; Temsamani, J.; Galbraith, W.; Tang, J. *Clin. Pharmacokinet.* **1995**, *28*, 7−16.
(25) Bijsterbosch, M. K.; Manoharan, M.; Rump, E. T.; De Vrueh, R. L.; van Veghel, R.; Tivel, K. L.; Biessen, E. A.; Bennett, C. F.; Cook, P. D.; van Berkel, T. J. *Nucleic Acids Res.* **1997**, *25*, 3290−3296.
(26) DeLong, R. K.; Nolting, A.; Fisher, M.; Chen, Q.; Wickstrom, E.; Kligshteyn, M.; Demirdji, S.; Caruthers, M.; Juliano, R. L. *Antisense Nucleic Acid Drug Dev.* **1997**, *7*, 71−77.
(27) Zendegui, J. G.; Vasquez, K. M.; Tinsley, J. H.; Kessler, D. J.; Hogan, M. E. *Nucleic Acids Res.* **1992**, *20*, 307−314.
(28) Geary, R. S.; Leeds, J. M.; Fitchett, J.; Burckin, T.; Truong, L.; Spainhour, C.; Creek, M.; Levin, A. A. *Drug Metab. Dispos.* **1997**, *25*, 1272−1281.
(29) Rifai, A.; Brysch, W.; Fadden, K.; Clark, J.; Schlingensiepen, K. H. *Am. J. Pathol.* **1996**, *149*, 717−725.
(30) Phillips, J. A.; Craig, S. J.; Bayley, D.; Christian, R. A.; Geary, R.; Nicklin, P. L. *Biochem. Pharmacol.* **1997**, *54*, 657−668.
(31) Garcia-Banuelos, J.; Siller-Lopez, F.; Miranda, A.; Aguilar, L. K.; Aguilar-Cordova, E.; Armendariz-Borunda, J. *Gene Ther.* **2002**, *9*, 127−134.
(32) Steward, A.; Christian, R. A.; Hamilton, K. O.; Nicklin, P. L. *Biochem. Pharmacol.* **1998**, *56*, 509−516.
(33) Emlen, W.; Rifai, A.; Magilavy, D.; Mannik, M. *Am. J. Pathol.* **1988**, *133*, 54−60.
(34) Takakura, Y.; Mahato, R. I.; Yoshida, M.; Kanamaru, T.; Hashida, M. *Antisense Nucleic Acid Drug Dev.* **1996**, *6*, 177−183.
(35) Yamasaki, Y.; Sumimoto, K.; Nishikawa, M.; Yamashita, F.; Yamaoka, K.; Hashida, M.; Takakura, Y. *J Pharmacol. Exp. Ther.* **2002**, *301*, 467−477.
(36) Butler, M.; Crooke, R. M.; Graham, M. J.; Lemonidis, K. M.; Lougheed, M.; Murray, S. F.; Witchell, D.; Steinbrecher, U.; Bennett, C. F. *J. Pharmacol. Exp. Ther.* **2000**, *292*, 489−496.
(37) Ye, Z.; Cheng, K.; Guntaka, R. V.; Mahato, R. I. *Biochemistry*, in press.

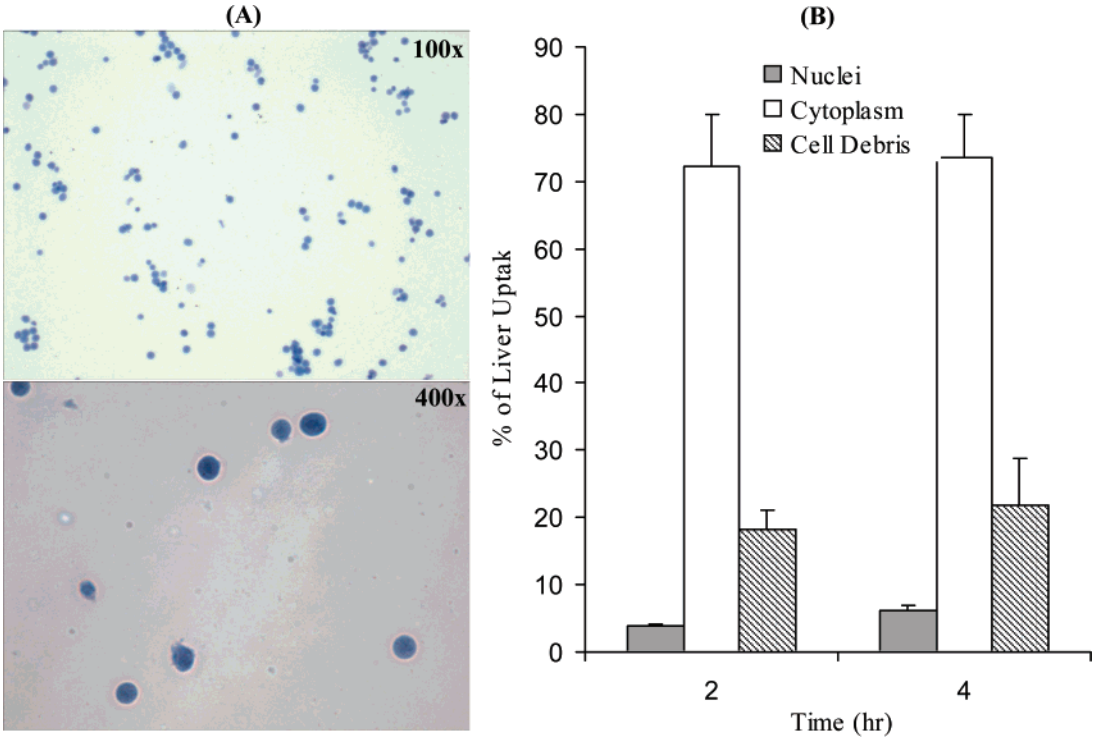

Figure 8. Subcellular distribution of ^{33}P-TFO in the liver at 2 and 4 h after intravenous administration in rats at doses of 1 mg/kg. Highly purified nuclei were isolated from cytoplasm and cell debris using the sucrose gradient separation method. The purity and number of isolated nuclei were determined under microscopy by dilution in trypan blue solution (A). TFO distributions in the nuclei, cytoplasm and cell debris were given as % of the total liver recovery (B). Data are presented as the mean ± SE ($n = 4$).

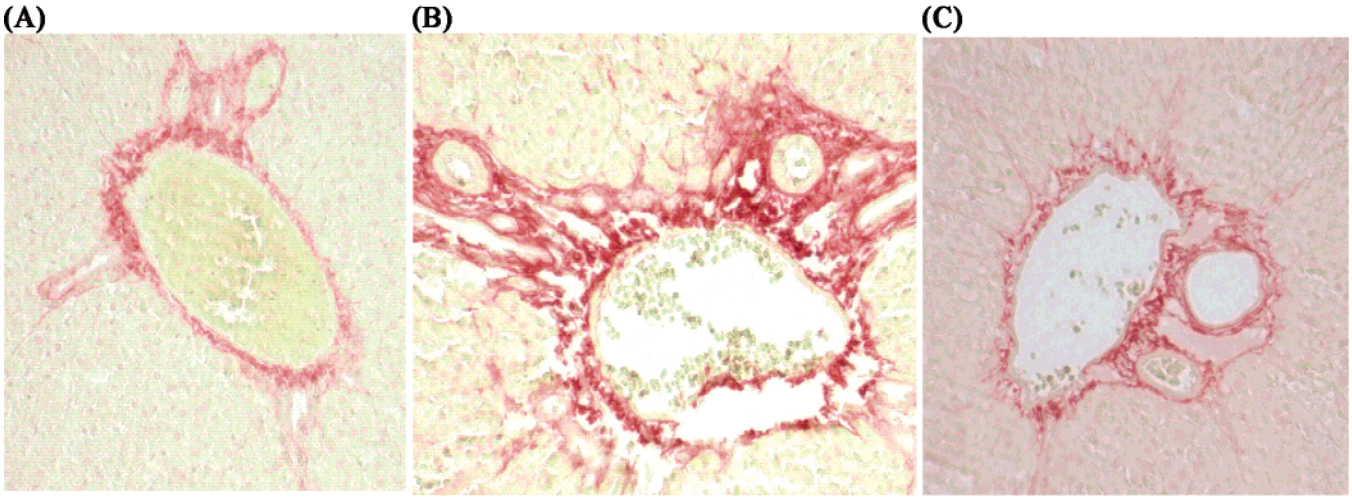

Figure 9. Effect of TFO on liver fibrosis. Liver fibrosis was induced by injection of 1% DMN in Sprague−Dawley male rats intraperitoneally at a dose of 1 mL/kg of body weight for 3 consecutive days per week for 5 weeks. TFO was injected intraperitoneally at a dose of 4 mg/kg of body weight every alternate day from the second week. After 5 weeks, all rats were sacrificed and livers were harvested and fixed in 10% formalin for histochemical staining with 0.1% Sirius red. (A) Controlled liver. (B) DMN-induced fibrotic liver. (C) DMN-induced fibrotic liver with treatment of TFO.

in vitro is mediated by a specific receptor whose characteristics are similar to those of the scavenger receptor. Graham et al.[8] concluded that almost 80% of injected PS ODNs are taken up by Kupffer and endothelial cells. The remaining 20% of the dose is taken up by the hepatocytes. Bijsterbosch et al. (2001) also reported that almost 70% of the liver recovery was associated with nonparenchymal cells like endothelial and Kupffer cells.[38] However, these authors did not isolate HSCs and thus the reported uptake of PS ODNs by Kupffer and endothelial cells may be an overestimate.

Since HSCs are the key fibrogenic cells responsible for the synthesis of ECM components, we isolated HSCs from Kupffer and endothelial cells by fractionation on Nycodenz gradient.[14] We had also ensured the purity of HSCs by staining of HSCs with desmin antibodies. In the liver, nonparenchymal cells such as HSCs, Kupffer cells, and endothelial cells showed the highest uptake, accounting for approximately 65−70% of the liver uptake (Figure 7B). At a 1 mg/kg dose, the TFO concentration in different liver cells was in the following order: 1342.41, 1433.19, and 100 ng/mg of cell protein for the HSCs, Kupffer and endothelial cells, and hepatocytes, respectively (Figure 7A). TFO concentration in these cells was significantly increased as we increased the dose of ^{33}P-TFO from 0.2 to 1 mg/kg (Figure 7A). Almost 40% of the total liver recovery was in the HSCs, 30% in the mixture of Kupffer and endothelial cell preparations, and the remaining 30% in the hepatocytes (Figure 7B). In a separate study, we recently conjugated mannose-6-phosphate bovine serum albumin (M6P-BSA) to the TFO via a disulfide bond and demonstrated enhanced TFO delivery to the HSCs.[39]

Since the TFO has to enter the nucleus to inhibit transcription of α1(I) collagen gene transcription, we determined the subcellular distribution of this TFO in the cytoplasm and nuclear extracts after isolation of highly purified nuclei from the liver. The nuclear distribution of the TFO was only 6.28 ± 0.59% at 4 h after systemic administration (Figure 8B), which is an underestimate since we could isolate only 42−45% of the liver cell nuclei. The overall nuclear distribution of the TFO in the liver cells is likely to be as high as 14.11 ± 2.04% at 4 h. Since the TFO targets only two alleles of type α1(I) collagen gene existing per cell, even a small % of the TFO which could traffic to the nucleus has a high potential to block type α1(I) collagen expression. Although we isolated nuclei from the whole liver rather than from different isolated liver cell types, we think that nuclear distribution of the TFO is mainly in the liver nonparenchymal cells and little in the hepatocytes as demonstrated by Graham et al. for PS ODNs.[8]

To determine the effect of TFO on the inhibition of α1(I) collagen, we stained the liver sections with Sirius red. The liver sections of TFO treated fibrotic rat liver showed collagen deposition higher than that of the control liver, but much lower than that of the DMN-treated rat liver (Figure 9). This suggests that, following systemic administration, the TFO could reach the liver cells and traffic to the nucleus where it inhibits the collagen transcription. Further experiments to determine the specific effect on α1(I) collagen are in progress.

To determine the effect of the TFO on liver fibrosis, we injected TFO intraperitoneally into the rats. Our preliminary data as well as the results from other laboratories[40] clearly suggest that ODNs could be taken up by the liver after intraperitoneal injection at high ratio and the distribution profile is similar to that of intravenous injection. Goodarzi et al.[41] also demonstrated that the hepatic uptake of ODNs was higher than the uptake for other organs regardless of the route of administration. Currently, we are evaluating the TFO effect on liver fibrosis after intravenous injection at different doses and frequencies of administration. These results will be reported in our subsequent publications.

In conclusion, ^{33}P-TFO is widely distributed to most peripheral tissues after systemic administration. A significant amount of TFO was taken up by HSCs and traffic to the liver nuclei. Therefore, we believe that our APS TFO against type α1(I) collagen promoter can be used for the treatment of liver fibrosis.

Abbreviations Used

APS, antiparallel phosphorothioate; AUC, area under the curve; CL, clearance; DMN, dimethylnitrosamine; ECM, extracellular matrix; HSCs, hepatic stellate cells; MRT, mean residence time; ODNs, oligodeoxynucleotides; polyC, polycytidylic acid; polyI, polyinosinic acid; PS, phosphorothioate; TFO, triplex-forming oligonucleotide; NPC, nonparenchymal cells; V_d, volume of distribution.

Acknowledgment. This work was supported by Grant RO1 DK 064366 from the NIH and USPHS Grant AR47379.

MP050012X

(38) Bijsterbosch, M. K.; Manoharan, M.; Dorland, R.; Waarlo, I. H.; Biessen, E. A.; van Berkel, T. J. *Biochem. Pharmacol.* **2001**, *62*, 627−633.

(39) Ye, Z.; Cheng, K.; Guntaka, R. V.; Mahato, R. I. *Biochemistry* **2005**, *44*, 4466−4476.

(40) Agrawal, S.; Temsamani, J.; Tang, J. Y. *Proc. Natl. Acad. Sci. U.S.A.* **1991**, *88*, 7595−7599.

(41) Goodarzi, G.; Watabe, M.; Watabe, K. *Biopharm. Drug Dispos.* **1992**, *13*, 221−227.